PHYSICAL REVIEW A **93**, 060301(R) (2016)

Fock-state stabilization and emission in superconducting circuits using dc-biased Josephson junctions

J.-R. Souquet and A. A. Clerk
Department of Physics, McGill University, 3600 rue University, Montreal, Quebec, Canada H3A 2T8
(Received 1 February 2016; published 21 June 2016)

We present and analyze a reservoir-engineering approach to stabilizing Fock states in a superconducting microwave cavity which does not require any microwave-frequency control drives. Instead, our system makes use of a Josephson junction biased by a dc voltage which is coupled to both a principal storage cavity and a second auxiliary cavity. Our analysis shows that Fock states can be stabilized with an extremely high fidelity. We also show how the same system can be used to prepare on-demand propagating Fock states, again without the use of microwave pulses.

DOI: 10.1103/PhysRevA.93.060301

Introduction. The ability to prepare, stabilize, and, ultimately, transmit nontrivial quantum states is crucial to a variety of tasks in quantum information processing [1]. In the presence of dissipation, state stabilization can be accomplished either via measurement-plus-feedback schemes (see, e.g., [2–9]) or autonomously, using quantum reservoir engineering (QRE) techniques [10]. There has been considerable progress in implementing QRE ideas in superconducting circuits, including experiments which have stabilized qubit states [11–13] as well as photonic Fock states [14] inside microwave frequency cavities. These schemes are typically complex, requiring the use of several high-frequency microwave control tones.

In this work, we focus on the stabilization and emission of Fock states in superconducting quantum circuits. Such states have applications in quantum communication, cryptography, and information processing (see, e.g., [15]) and are a crucial ingredient in linear optical quantum computation [16]. We take an alternate approach here to Fock-state stabilization, which requires no high-frequency microwave control tones and only a dc voltage and a single Josephson junction. This leads to considerable simplicity over existing protocols and negates any issues involving the microwave control tones corrupting the generated Fock state (a problem that is typically solved by using elaborate fast frequency-tunable qubits [17,18]). Our approach also represents a fundamentally different approach to reservoir engineering which utilizes a highly nonlinear driving of a cavity, rather than nonlinear cavity-cavity interactions.

The starting point for our scheme is a setup discussed in a number of recent theoretical studies [19–21] and experiments [22–25], where a microwave cavity is coupled to a dc-biased Josephson junction. The driven junction does not act like a qubit, but rather as a highly nonlinear driving element. That such a setup can produce nonclassical photonic states was first pointed out in Ref. [20], which showed that states could be produced having suppressed number fluctuations and a vanishing $g^{(2)}$ intensity correlation function. While these states violate a classical Cauchy-Schwarz inequality, they are mixtures of the vacuum and the one-photon Fock state and have a limited fidelity with a pure Fock state [26]. As a result, they do not exhibit any negativity in their Wigner functions [27].

Here, we show how optimally coupling the junction to a second cavity (as depicted in Fig. 1) lets one transcend the limitations of the single-cavity system and prepare single-photon Fock states with an extremely high fidelity. In addition, it can easily be adapted to prepare higher Fock states. The second cavity acts like an engineered dissipative reservoir which freezes the system dynamics in the desired Fock state. Similar two-cavity-plus-junction systems have recently been realized experimentally [22] and have also been discussed theoretically [28–31], largely in the context of generating cavity-cavity correlations. Armour et *al.* [29] found numerically that such a system could generate cavity states with weakly negative Wigner functions; they did not, however, discuss Fock-state stabilization or the particular mechanism we elucidate and optimize.

In addition to efficient and high-fidelity Fock-state stabilization, we show that our setup can also play another crucial role: it can act as an efficient means for producing propagating Fock states on demand. In circuit QED setups, propagating single-photon states are usually generated by driving microwave cavities coupled to a qubit with high-frequency control pulses (see, e.g., [32]). Among the many challenges in the standard approach is the requirement that the generated photon should be far detuned from the frequency of the control pulse [17,18,33]. Our system is capable of on-demand Fock-state generation without any microwave control pulses: one simply needs to pulse a dc control voltage. We note that recent work by Leppäkangas *et al.* studied an alternative approach to generating propagating single photons using a biased Josephson junction [34,35]. Contrary to our work, this setup is based on using Coulomb blockade physics and does not lead to the stabilization of an intracavity Fock state; it also does not allow for the production of higher Fock states.

Biased junction as a nonlinear drive. To set the stage for our two-cavity system, we start by quickly reviewing the physics of the one-cavity version, as studied in [19,20]. The system consists of a Josephson junction in series with a LC resonator (frequency ω_c, impedance Z) and a dc voltage source V_{dc}. We focus exclusively on temperature and voltages small enough that superconducting quasiparticles are never excited. The Hamiltonian has the form $\hat{H} = \omega_c(\hat{a}^\dagger\hat{a} + 1/2) - E_J\cos(\hat{\phi})$, where $\hat{a}$ is the cavity photon annihilation operator, E_J is the Josephson energy, and $\hat{\phi}$ is the phase difference across the junction; unless otherwise noted, we set $\hbar = 1$ throughout.

 ©2016 American Physical Society

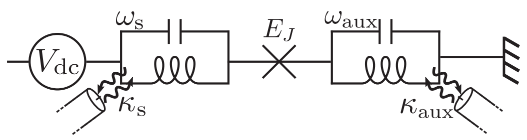

FIG. 1. Schematic of the proposed setup. A dc-biased Josephson junction of energy E_J is in series with two cavities. Each cavity has an impedance close to $R_K = h/e^2$ and is damped via a coupling to a transmission line.

The voltage drop across the junction $d\hat{\phi}/dt$ is given by the difference of V_{dc} and the cavity voltage $\hat{V}_{cav}$. This leads to $\hat{\phi} = 2[eV_{dc}t + \lambda(\hat{a} + \hat{a}^\dagger)]$, where $\lambda = \sqrt{\pi Z/R_K}$ sets the magnitude of the cavity's zero-point flux fluctuations and $R_K = h/e^2$ is the resistance quantum. The cavity is also coupled to a transmission line, which is treated (as standard) as a Markovian reservoir and which gives rise to an energy damping rate κ. Working in an interaction picture at the cavity frequency, the Hamiltonian of the cavity plus biased junction takes the form [19,20,30,36–38]

$$\hat{H} = -\frac{E_J}{2}(e^{2ieV_{dc}t}\hat{D}[\alpha(t)] + e^{-2ieV_{dc}t}\hat{D}^\dagger[\alpha(t)]), \quad (1)$$

where $\hat{D}[\alpha(t)]$ is the cavity displacement operator [corresponding to a time-dependent displacement $\alpha(t)$]. It is defined in terms of the photon annihilation operator $\hat{a}$ as

$$\hat{D}[\alpha(t)] = e^{\alpha(t)\hat{a}^\dagger - \alpha^*(t)\hat{a}}, \ \alpha(t) = 2\lambda e^{i\omega_c t}. \quad (2)$$

Note that we consider the case where intrinsic phase fluctuations of the junction (due to charging effects or noise from a shunt resistor) play no role. For more details on the derivation of this Hamiltonian, see, e.g., Refs. [19,20].

From the point of view of the cavity, $\hat{H}$ describes a highly nonlinear (but coherent) cavity drive [20]: each term tunnels a Cooper pair and also displaces the cavity state by $\pm\alpha(t)$. To see clearly how these displacements can result in Fock-state generation, we follow a different route from [20] and express $\hat{D}[\alpha(t)]$ directly in the Fock basis (see, e.g., [39]):

$$\hat{D}[\alpha(t)] = \sum_{n=0}^{\infty}\sum_{l=0}^{\infty} w_{n,n+l}[\lambda]\,|n\rangle\langle n+l|e^{-il\omega_c t} + \sum_{l=1}^{\infty}(-1)^l|n+l\rangle\langle n|w_{n+l,n}[\lambda]e^{il\omega_c t}. \quad (3)$$

Here, the transition amplitude $w_{n,n+l}[\lambda]$ is nothing more than a generalized Frank-Condon factor. For $l \geqslant 0$ we have

$$w_{n+l,n}[\lambda] = e^{-2\lambda^2}(2\lambda)^l\sqrt{\tfrac{n!}{(n+l)!}}L_n^{(l)}(4\lambda^2), \quad (4)$$

where $L_n^{(k)}$ is a Laguerre polynomial [40] and $w_{n+l,n}[\lambda] = w_{n,n+l}[-\lambda]$.

As is well known, Frank-Condon factors are highly nonlinear functions of the magnitude of the displacement (here set by λ) and can even exhibit zeros [41] corresponding to zeros of the Laguerre polynomials; the behavior of relevant factors is shown in Fig. 2. We let $\tilde{\lambda}_{n+l,n}$ denote the smallest value of λ which makes $w_{n+l,n}[\lambda]$ vanish:

$$w_{n+l,n}[\tilde{\lambda}_{n+l,n}] = w_{n,n+l}[\tilde{\lambda}_{n+l,n}] = 0. \quad (5)$$

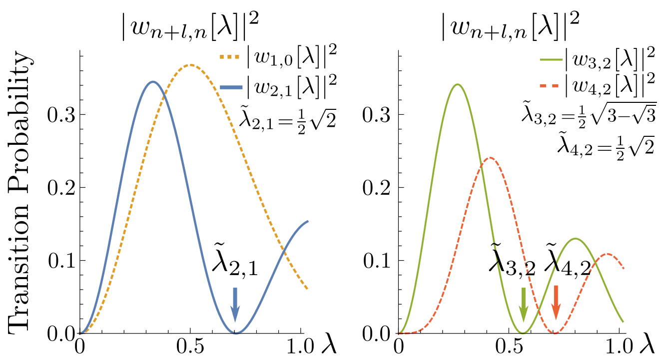

FIG. 2. Matrix elements $w_{n+l,n}[\lambda]$ for junction-driven cavity Fock-state transitions as a function of the zero-point voltage fluctuation amplitude λ for different values of n and l. These functions are highly nonlinear with respect to λ and can cancel for specific values. Roots of $w_{n+l,n}[\lambda]$, denoted $\tilde{\lambda}_{n+l,n}$, are indicated.

We note that in comparison to the Bessel function expansion used in Ref. [20], the decomposition in Eq. (3) makes it easier to identify values of λ yielding zeros and also highlights the direct connection to Franck-Condon physics.

The route to preparing single Fock states now seems clear: by tuning the value of both V_{dc} and λ (via the cavity impedance Z), one can arrange for the effective driving of the cavity by the junction to shut off when a given Fock state is reached [14]. For concreteness, suppose we chose $V_{dc} = k\Omega/2e$ (k an integer), so that to leading order, Cooper pairs can only tunnel by emitting or absorbing k cavity photons. If we take $\omega_c \gg E_J,\kappa$, we can restrict attention to these processes and make a rotating-wave approximation (RWA) to our full Hamiltonian. Within the RWA we have

$$\hat{H}_{RWA} = (-1)^{k+1}\frac{E_J}{2}\sum_{n=0}^{\infty} w_{n+k,n}[\lambda]|n+k\rangle\langle n| + \text{H.c.} \quad (6)$$

Consider the simplest case where $k = 1$, and each resonantly tunneling Cooper pair emits or absorbs a single cavity photon. If we then set $\lambda = 1/\sqrt{2} \equiv \tilde{\lambda}_{2,1}$ (see Fig. 2, left panel), there is no matrix element in Eq. (6) for a transition from one to two cavity photons. As first discussed in Ref. [20], the junction-induced drive now can add at most one photon to the cavity, implying that the system effectively acts like a driven two-level system.

The cavity steady state is found by solving the Lindblad master equation for the density matrix of the cavity $\hat{\rho}_c$ for $\dot{\hat{\rho}}_c = 0$,

$$\dot{\hat{\rho}}_c = -i[\hat{H}_{RWA},\hat{\rho}_c] + \kappa\mathcal{L}[\hat{a}]\hat{\rho}_c, \quad (7)$$

which includes the dissipation from the (zero-temperature) transmission line; here, $\mathcal{L}[\hat{a}]\hat{\rho} = \hat{a}\hat{\rho}\hat{a}^\dagger - \frac{1}{2}\{\hat{\rho}\hat{n} + \hat{n}\hat{\rho}\}$. Note this dissipator naturally implies that the lifetime of the nth Fock state decreases with n. When λ is set to $\tilde{\lambda}_{2,1}$, the stationary intracavity state can be termed nonclassical in that it results in a vanishing $g^{(2)}$ intensity-intensity correlation function [20]. This simply reflects the fact that there is zero probability for having two or more photons in the cavity. We are still far, however, from our goal of producing a single-photon Fock state. As the cavity is effectively a driven two-level system, population inversion is impossible, and at best the steady state is an incoherent mixture with an equal probability of vacuum and single photon. We stress that such a state exhibits no negativity in its Wigner function.

Fock-state stabilization. Heuristically, the poor performance of the single-cavity setup is easy to understand: even if we eliminate the matrix element for $|1\rangle \to |2\rangle$ transitions, the junction-driven cavity continues to oscillates back and forth between the vacuum and the $|1\rangle$ Fock state. To achieve true Fock-state generation, one needs to shut off the oscillation dynamics when the system is in the $|1\rangle$ state. As we now discuss, this can be achieved rather simply by coupling the junction to a second "auxiliary" cavity (see Fig. 1) whose damping rate $\kappa_{\rm aux}$ is taken to be sufficiently large. We have so far not included the effects of low-frequency voltage fluctuations on the dynamics. The primary effect of these fluctuations is to cause dephasing (see, e.g., Ref. [22]), causing coherences in the density matrix to decay. As these coherences already decay due to the large auxiliary cavity damping, we are relatively robust against this noise. This is discussed further (along with full master-equation simulations including dephasing) in the Supplemental Material [42].

In what follows, we denote quantities for the main "storage" cavity with a subscript s, while auxiliary cavity quantities have a subscript aux; Fock states of the two-mode system are denoted $|n,m\rangle = |n\rangle_{\rm s} \otimes |m\rangle_{\rm aux}$. Working in an interaction picture with respect to the free-cavity Hamiltonians, the system Hamiltonian is

$$\hat{\mathcal{H}} = -\tfrac{E_J}{2} e^{2ieV_{\rm dc}t} \hat{\mathcal{D}}[\alpha_{\rm s}(t),\alpha_{\rm aux}(t)] + \text{H.c.} \tag{8}$$

Here, $\hat{\mathcal{D}}[\alpha_{\rm s}(t),\alpha_{\rm aux}(t)] = \hat{D}_{\rm s}[\alpha_{\rm s}(t)] \otimes \hat{D}_{\rm aux}[\alpha_{\rm aux}(t)]$ is the tensor product of displacement operators for each cavity, with respective displacement amplitudes $\alpha_j(t) = 2\lambda_j e^{i\omega_j t}$.

For the auxiliary cavity to play the desired role, we tune the voltage so that $V_{\rm dc} = (\omega_{\rm s} + \omega_{\rm aux})/2e$. Cooper-pair tunneling thus requires simultaneously emitting a single photon to each cavity (or absorbing a photon from each cavity). We also tune the storage-cavity impedance so that $\lambda_{\rm s} = \tilde{\lambda}_{2,1}$. We choose $\lambda_{\rm aux}$ such that $w_{1,0}[\lambda_{\rm aux}]$ is large (see Fig. 2), but we stress that no special tuning of $\lambda_{\rm aux}$ is needed. The resulting dynamics is sketched in Fig. 3(b). Similar to the single-cavity system, the effective driving from the biased junction couples $|0,0\rangle$ to $|1,1\rangle$ but not to states with a higher photon number. We would seem yet again to have an effective two-level system and might expect coherent oscillations between these two states. However, the large damping rate $\kappa_{\rm aux}$ of the auxiliary cavity prevents this: if the system is in the $|1,1\rangle$ state, $\kappa_{\rm aux}$ will cause a rapid decay to $|1,0\rangle$. In the absence of storage-cavity damping, the system is then effectively stuck: Cooper-pair tunneling against the voltage is impossible (as there are no photons in the aux cavity), while tunneling with the voltage is impossible as there is no matrix element connecting $|1,0\rangle$ and $|2,1\rangle$. Including storage-cavity damping does not ruin the physics: if the storage-cavity photon leaks out, one is back in the vacuum state, and the process starts again. One thus sees the possibility for having a steady state that has a high fidelity with the state $|1,0\rangle$, i.e., a stabilized single-photon state in the storage cavity.

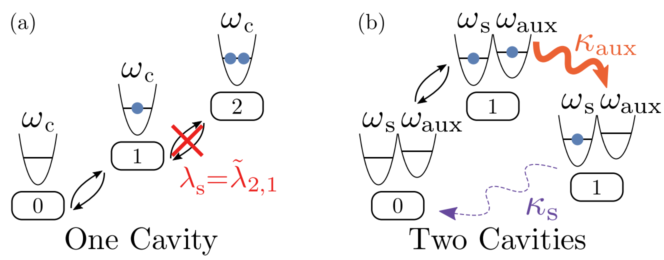

FIG. 3. Schematic depictions of biased-junction cavity pumping processes. The boxed digit indicates the number of Cooper pairs that have tunneled, whereas dots in the parabolas indicate the intracavity photon number. (a) Single-cavity setup for an impedance yielding $\lambda = \tilde{\lambda}_{2,1}$. Cooper-pair tunneling can take the cavity between the zero- and one-photon states, but transitions to the two-photon state are blocked. (b) Two-cavity setup for Fock-state stabilization, where $\lambda_{\rm s} = \tilde{\lambda}_{2,1}$. Starting from vacuum, Cooper-pair tunneling can cause oscillations between the $|0,0\rangle$ and $|1,1\rangle$ photon Fock states. Photon decay from the aux cavity, however, freezes the system into the desired $|1,0\rangle$ state. When the storage-cavity photon decays (due to $\kappa_{\rm s}$), the cycle repeats.

Let us make the above picture more quantitative. We start by applying the RWA to Eq. (8),

$$\hat{\mathcal{H}}_{\rm RWA} = \frac{E_J}{2}\left(\sum_{n_{\rm s}=0}^{\infty} w_{n_{\rm s}+1,n_{\rm s}}[\lambda]|n_{\rm s}+1\rangle\langle n_{\rm s}|\right) \otimes \left(\sum_{n_{\rm aux}=0}^{\infty} w_{n_{\rm aux}+1,n_{\rm aux}}[\lambda]|n_{\rm aux}+1\rangle\langle n_{\rm aux}|\right) + \text{H.c.} \tag{9}$$

Each cavity is also coupled to its own zero-temperature bath, and the reduced density matrix $\hat{\rho}$ of the two cavities obeys the Lindblad master equation:

$$\dot{\hat{\rho}} = -i[\hat{H}_{\rm RWA},\hat{\rho}] + \kappa_{\rm aux}\mathcal{L}[\hat{a}_{\rm aux}]\hat{\rho} + \kappa_{\rm s}\mathcal{L}[\hat{a}_{\rm s}]\hat{\rho}. \tag{10}$$

Consider first the ideal case, where $\lambda_{\rm s}$ is tuned perfectly to equal $\tilde{\lambda}_{2,1}$. In the relevant limit $\kappa_{\rm s} \ll \kappa_{\rm aux}$, the steady-state probability that the system is in the desired state $|1,0\rangle$ is

$$\langle 1,0|\hat{\rho}|1,0\rangle \simeq \frac{\Gamma}{\Gamma+\kappa_{\rm s}}, \quad \Gamma = \frac{(E_J w_{1,0}[\lambda_{\rm s}] w_{1,0}[\lambda_{\rm aux}])^2}{\kappa_{\rm aux}}, \tag{11}$$

where Γ plays the role of an effective pumping rate from $|0,0\rangle$ to $|1,0\rangle$ and we have dropped terms as small as $\kappa_{\rm s}/\kappa_{\rm aux}$. The probability to be in the desired state tends to 1 in the limit $\Gamma \gg \kappa_{\rm aux} \gg \kappa_s$. The large $|1,0\rangle$ population here is analogous to the population inversion possible in a driven three-level system [43]. We note in passing that the fidelity between the state of the storage cavity and the desired $|1\rangle$ Fock state is just given by the probability to have a single photon [26]; hence, the above expression is a lower bound on the fidelity.

The above process can be efficient even if the storage-cavity impedance is not perfectly tuned. Suppose $\lambda_{\rm s} = \tilde{\lambda}_{2,1} + \varepsilon$ with $\varepsilon \ll 1$. Assuming again $\kappa_{\rm s} \ll \kappa_{\rm aux}$, one finds that the

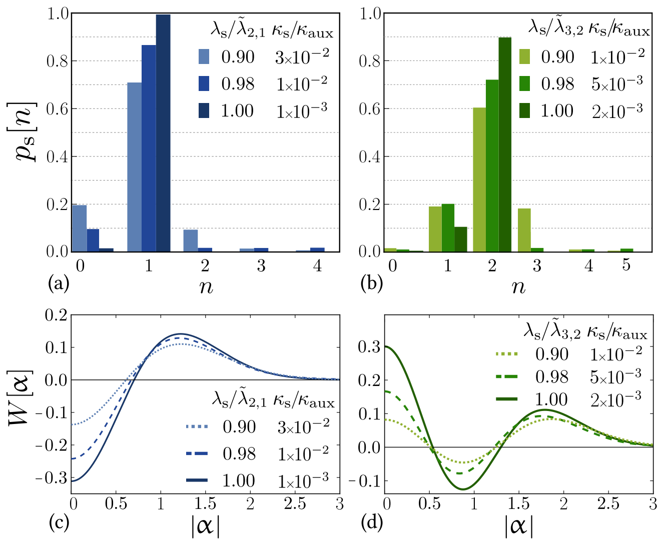

FIG. 4. Steady-state probability $p_s[n]$ for the storage cavity to be in a Fock state $|n\rangle_s$, as obtained from the RWA master equation in Eq. (10). We take $E_J = \kappa_{aux} \ll \omega_s, \omega_{aux}$, and $\lambda_{aux} = 1/2$; λ_s and κ_s are indicated in the plots. For each n, the rightmost bar represents λ closest to perfect tuning. (a) Probabilities when λ_s is tuned close to $\tilde{\lambda}_{2,1}$ (for stabilizing $|1\rangle$). (b) The same for λ_s tuned close to $\tilde{\lambda}_{3,2}$ (for stabilizing $|2\rangle$). Even with imperfect tuning, the target Fock state is stabilized with a high fidelity. (c) and (d) Corresponding Wigner function $W[\alpha]$ for the storage-cavity state, showing that negative values are obtained; note that $W[\alpha]$ is rotationally invariant in all cases.

probability to be in $|1,0\rangle$ is modified to be

$$\langle 1,0|\hat{\rho}|1,0\rangle \simeq \frac{\Gamma}{\Gamma + \kappa_s + 4\varepsilon^2\Gamma^2/\kappa_s}. \tag{12}$$

Because of the imperfect tuning of λ_s, it is no longer advantageous to have $\Gamma \gg \kappa_s$ (i.e., large E_J), as transitions to higher states will corrupt the dynamics. Equation (12) suggests that an optimal choice would be to have $\kappa_s = 2\varepsilon\Gamma$ (while still maintaining $\kappa_{aux} \gg \kappa_s$).

To complement the above analytical results, we have performed a full numerical simulation of the RWA master equation in Eq. (10) using the QUTIP package [44]. Figure 4(a) shows the stationary storage-cavity photon-number distribution for different choices of λ_s. The probability to be in the desired $|1\rangle$ Fock state is ~0.70 even with a 10% mismatch between λ_s and its ideal value and jumps to ~0.86 if the mismatch is reduced to 2%. These fidelities are high enough to give rise to storage-cavity Wigner functions that exhibit large amounts of negativity [as shown in Fig. 4(c)]. They also compare favorably both to the single-cavity scheme of Ref. [20] (where even in the ideal case the fidelity can never be greater than 0.5 and negative Wigner functions are impossible) and to Ref. [14], where the experimentally measured fidelity was ~0.67.

Our protocol can also be used to stabilize higher Fock states with a good fidelity. One keeps the voltage set to $V_{dc} = (\omega_s + \omega_{aux})/2e$ but now tunes the storage-cavity impedance such that $\lambda_s = \tilde{\lambda}_{n+1,n}$ for some chosen $n > 1$. The system dynamics will now effectively get stuck in the state $|n,0\rangle$. Numerical results for the case $n = 2$ are shown in Figs. 4(b) and 4(d).

We stress that the general scheme here can be viewed as an example of reservoir engineering [10], with the biased junction and auxiliary cavity acting as an effective dissipative environment which stabilizes the storage cavity in the desired Fock state. In that respect, our protocol has similarities to the Fock-state stabilization scheme described and implemented in Ref. [14]. In that work, the engineered reservoir also involved an auxiliary cavity but used a qubit and two microwave control tones (or more if the target Fock state had $n > 1$). In our work, the auxiliary cavity is still there, but the microwave control tones and qubit have been replaced with a Josephson junction biased by a dc voltage. Note that conversely to Ref. [14], reaching higher Fock states does not require additional resources.

Itinerant Fock states on demand. The above protocol for stabilizing Fock states can naturally be used to produce propagating Fock states: after the desired Fock state has been stabilized, one simply turns off the dc bias voltage when the itinerant photon is desired, and the storage-cavity Fock state will be emitted into the transmission line coupled to it (in a temporal mode with an exponential profile [45,46]). An alternate strategy is to exploit the transient dynamics of our scheme and produce an itinerant Fock state with a pulsed dc voltage. In this case, one optimizes parameters to have a high-fidelity intracavity Fock state at an intermediate time, as opposed to in the long-time steady state. The voltage is then turned off at this intermediate time. This makes it possible to achieve a high-fidelity Fock state even if the tuning of

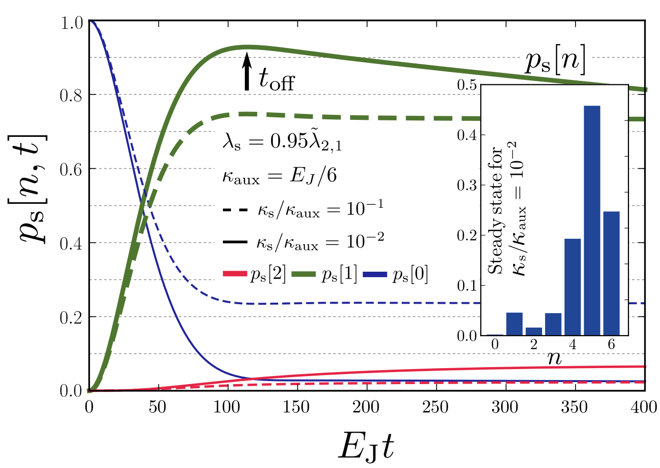

FIG. 5. Time dependence of storage-cavity photon-number occupancies $p_s[n,t]$, where the bias $V_{dc} = (\omega_{aux} + \omega_s)/2e$ is turned on at $t = 0$ and the cavities start from vacuum. Dashed line: κ_s chosen to optimize the steady-state value of $p_s[1,t]$ (thick dashed line) with the Fock-state stabilization protocol. Solid line: alternate choice of κ_s which optimize $p_s[1,t]$ (thick solid line) at intermediate times with the pulsed protocol. In this latter protocol, the voltage can be turned off near t_{off}, resulting with high probability in the production of a propagating Fock state in the transmission line coupled to the storage cavity. In both cases, we assume the realistic situation where the cavity impedance has not been tuned perfectly (here, $\lambda_s = 0.95\tilde{\lambda}_{21}$ and $\lambda_{aux} = 0.13\tilde{\lambda}_{21}$). The inset shows $p_s[n,t \to \infty]$ for the pulsed protocol.

the storage-cavity impedance is not perfect, i.e., $\lambda_s \neq \tilde{\lambda}_{2,1}$. In addition, by choosing parameters such that the oscillation dynamics associated with Cooper-pair tunneling is slightly overdamped, one can have a protocol which is relatively insensitive to the timing of the voltage pulse.

In Fig. 5, we show a comparison between the steady-state stabilization protocol and this pulsed protocol, where λ_s deviates by 5% from the ideal value $\tilde{\lambda}_{2,1}$ needed for single-photon generation. By using a value of κ_s smaller than the choice that optimizes the steady-state single-photon probability, one obtains a much higher fidelity with a single-photon Fock state at intermediate times. We find that at an optimal turnoff time, a state fidelity of $\sim$0.92 with the $|1\rangle$ Fock state can be obtained (see thick solid line in Fig. 5). Further, the maximum probability for having a single storage-cavity photon is a rather broad function of time, meaning that one does not need precise control of the shutoff time of the dc voltage. This is in stark contrast to standard protocols for preparing a Fock state using two-level system dynamics (e.g., in the one-cavity version of our system), where one needs precise control of the duration of the pulses control.

Note that in the above simulations, the voltage is abruptly turned on. More realistic situations where the voltage is slowly ramped on yield a similar result as the tunneling processes are resonant only when $2eV \simeq \Omega_{\mathrm{aux}} + \Omega_s$.

Conclusion. We have shown how a system where a voltage-biased Josephson junction is coupled to two cavities can be used to stabilize Fock states with a high efficiency. While our approach does require one to carefully tune the impedance of the main storage cavity, it does not require any microwave-frequency control tones. We also discussed how the same setup could be used to produce itinerant single photons on demand.

Acknowledgments. This work was supported by NSERC. We acknowledge fruitful discussions with P. Hofer, M. Hofheinz, F. Portier, and J. Viennot.

[1] T. D. Ladd, F. Jelezko, R. Laflamme, Y. Nakamura, C. Monroe, and J. L. O' Brien, Nature (London) **464**, 45 (2010).
[2] A. R. Calderbank and P. W. Shor, Phys. Rev. A **54**, 1098 (1996).
[3] R. J. Nelson, Y. Weinstein, D. Cory, and S. Lloyd, Phys. Rev. Lett. **85**, 3045 (2000).
[4] W. P. Smith, J. E. Reiner, L. A. Orozco, S. Kuhr, and H. M. Wiseman, Phys. Rev. Lett. **89**, 133601 (2002).
[5] R. L. Cook, P. J. Martin, and J. M. Geremia, Nature (London) **446**, 774 (2007).
[6] G. G. Gillett, R. B. Dalton, B. P. Lanyon, M. P. Almeida, M. Barbieri, G. J. Pryde, J. L. O'Brien, K. J. Resch, S. D. Bartlett, and A. G. White, Phys. Rev. Lett. **104**, 080503 (2010).
[7] C. Sayrin, I. Dotsenko, X. Zhou, B. Peaudecerf, T. Rybarczyk, S. Gleyzes, P. Rouchon, M. Mirrahimi, H. Amini, M. Brune *et al.*, Nature (London) **477**, 73 (2011).
[8] R. Vijay, C. Macklin, D. Slichter, S. Weber, K. Murch, R. Naik, A. N. Korotkov, and I. Siddiqi, Nature (London) **490**, 77 (2012).
[9] D. Riste, M. Dukalski, C. Watson, G. de Lange, M. Tiggelman, Y. M. Blanter, K. Lehnert, R. Schouten, and L. DiCarlo, Nature (London) **502**, 350 (2013).
[10] J. F. Poyatos, J. I. Cirac, and P. Zoller, Phys. Rev. Lett. **77**, 4728 (1996).
[11] K. W. Murch, U. Vool, D. Zhou, S. J. Weber, S. M. Girvin, and I. Siddiqi, Phys. Rev. Lett. **109**, 183602 (2012).
[12] S. Shankar, M. Hatridge, Z. Leghtas, K. Sliwa, A. Narla, U. Vool, S. M. Girvin, L. Frunzio, M. Mirrahimi, and M. H. Devoret, Nature (London) **504**, 419 (2013).
[13] M. E. Schwartz, L. Martin, E. Flurin, C. Aron, M. Kulkarni, H. E. Tureci, and I. Siddiqi, arXiv:1511.00702.
[14] E. T. Holland, B. Vlastakis, R. W. Heeres, M. J. Reagor, U. Vool, Z. Leghtas, L. Frunzio, G. Kirchmair, M. H. Devoret, M. Mirrahimi, and R. J. Schoelkopf, Phys. Rev. Lett. **115**, 180501 (2015).
[15] B. Lounis and M. Orrit, Rep. Prog. Phys. **68**, 1129 (2005).
[16] E. Knill, R. Laflamme, and G. J. Milburn, Nature (London) **409**, 46 (2001).
[17] C. Eichler, D. Bozyigit, C. Lang, L. Steffen, J. Fink, and A. Wallraff, Phys. Rev. Lett. **106**, 220503 (2011).
[18] W. F. Kindel, M. D. Schroer, and K. W. Lehnert, Phys. Rev. A **93**, 033817 (2016).
[19] A. D. Armour, M. P. Blencowe, E. Brahimi, and A. J. Rimberg, Phys. Rev. Lett. **111**, 247001 (2013).
[20] V. Gramich, B. Kubala, S. Rohrer, and J. Ankerhold, Phys. Rev. Lett. **111**, 247002 (2013).
[21] S. Dambach, B. Kubala, V. Gramich, and J. Ankerhold, Phys. Rev. B **92**, 054508 (2015).
[22] M. Hofheinz, F. Portier, Q. Baudouin, P. Joyez, D. Vion, P. Bertet, P. Roche, and D. Estève, Phys. Rev. Lett. **106**, 217005 (2011).
[23] F. Chen, J. Li, A. D. Armour, E. Brahimi, J. Stettenheim, A. J. Sirois, R. W. Simmonds, M. P. Blencowe, and A. J. Rimberg, Phys. Rev. B **90**, 020506 (2014).
[24] C. Altimiras, O. Parlavecchio, P. Joyez, D. Vion, P. Roche, D. Esteve, and F. Portier, Appl. Phys. Lett. **103**, 212601 (2013).
[25] N. Samkharadze, A. Bruno, P. Scarlino, G. Zheng, D. DiVincenzo, L. DiCarlo, and L. M. K. Vandersypen, Phys. Rev. Applied **5**, 044004 (2016).
[26] A. Uhlmann, Rep. Math. Phys. **9**, 273 (1976).
[27] T. Hakiogammalu and A. S. Shumovsky, *Quantum Optics and the Spectroscopy of Solids: Concepts and Advances*, Fundamental Theories of Physics Vol. 83 (Springer, Dordrecht, 2013).
[28] J. Leppäkangas, G. Johansson, M. Marthaler, and M. Fogelström, Phys. Rev. Lett. **110**, 267004 (2013).
[29] A. D. Armour, B. Kubala, and J. Ankerhold, Phys. Rev. B **91**, 184508 (2015).
[30] M. Trif and P. Simon, Phys. Rev. B **92**, 014503 (2015).
[31] P. P. Hofer, J.-R. Souquet, and A. A. Clerk, Phys. Rev. B **93**, 041418 (2016).
[32] A. A. Houck, D. I. Schuster, J. M. Gambetta, J. A. Schreier, B. R. Johnson, J. M. Chow, L. Frunzio, J. Majer, M. H. Devoret, S. M. Girvin *et al.*, Nature (London) **449**, 328 (2007).
[33] M. Pechal, L. Huthmacher, C. Eichler, S. Zeytinoglu, A. A. Abdumalikov, S. Berger, A. Wallraff, and S. Filipp, Phys. Rev. X **4**, 041010 (2014).
[34] J. Leppäkangas, M. Fogelström, M. Marthaler, and G. Johansson, Phys. Rev. B **93**, 014506 (2016).

[35] J. Leppäkangas, M. Fogelström, A. Grimm, M. Hofheinz, M. Marthaler, and G. Johansson, Phys. Rev. Lett. **115**, 027004 (2015).

[36] S. Meister, M. Mecklenburg, V. Gramich, J. T. Stockburger, J. Ankerhold, and B. Kubala, Phys. Rev. B **92**, 174532 (2015).

[37] G.-L. Ingold, Y. V. Nazarov, H. Grabert, and M. Devoret, in *Single Charge Tunneling: Coulomb Blockade Phenomena in Nanostructures*, *NATO Advanced Studies Institute, Series B: Physics* Vol. 294 (Plenum, New York, 1992), p. 21.

[38] M. H. Devoret, in *Fluctuations Quantiques*, *Les Houches, Session LXIII, 1995* (Elsevier, Amsterdam, 1997), p. 7.

[39] K. E. Cahill and R. Glauber, Phys. Rev. **177**, 1857 (1969).

[40] By convention, $1/(l+n)! = 0$ for $l+n<0$.

[41] W. Smith, J. Phys. B **1**, 89 (1968).

[42] See Supplemental Material at http://link.aps.org/supplemental/10.1103/PhysRevA.93.060301 for further information on the effects of dephasing due to low-frequency voltage noise (including full master-equation simulations).

[43] D. F. Walls and G. J. Milburn, *Quantum Optics* (Springer, Berlin, 2007).

[44] J. Johansson, P. Nation, and F. Nori, Comput. Phys. Commun. **184**, 1234 (2013).

[45] Y. Yin, Y. Chen, D. Sank, P. O'Malley, T. White, R. Barends, J. Kelly, E. Lucero, M. Mariantoni, A. Megrant *et al.*, Phys. Rev. Lett. **110**, 107001 (2013).

[46] D. Maxwell, D. J. Szwer, D. Paredes-Barato, H. Busche, J. D. Pritchard, A. Gauguet, K. J. Weatherill, M. P. A. Jones, and C. S. Adams, Phys. Rev. Lett. **110**, 103001 (2013).

Supplemenary material for "Fock-state stabilization and emission in superconducting circuits using dc-biased Josephson junctions"

J.-R. Souquet, A. A. Clerk
Department of Physics, McGill University, 3600 rue University, Montreal, Quebec, H3A 2T8, Canada
(Dated: May 25, 2016)

In this supplemental section, we study the effects of decoherence due to voltage fluctuations from the low-frequency environment and show that they have a rather limited impact on the results presented in the main text. The low-frequency voltage fluctuations can be well-modelled as stemming from an environment with a roughly frequency-independent impedance at relevant frequencies [**?** **?**]. For temperatures $T > \omega$, the spectral density of the voltage fluctuations are then given by $S[\omega] \simeq 2Zk_BT$ with Z the impedance of the low frequency environment (see, e.g., [**?**]).

As typical dephasing rates due to the voltage noise are worst comparable to T, we can safely use a Markovian approximation to describe the voltage-noise induced dephasing (i.e. effectively treat the spectral density as being white). We note that in the experiment of Ref.[**?**] (which had relatively large amounts of voltage noise), the dephasing rate due to voltage noise was estimated as $\Gamma_\varphi \sim 150$ MHz. In this worst-case scenario, a white noise approximation should be safe for temperatures down to $\sim$ 75 mK. Within the white noise approximation, the dephasing rate is simply given by $\Gamma_\varphi = S[0]$. Note even using the numbers from Ref.[**?**], this rate is much smaller than the Josephson energy and the auxiliary cavity damping rate we used in our simulations ($E_J = \kappa_{\rm aux} \simeq 1$GHz).

To include the voltage-noise dephasing in our master equation treatment, we start by adding a classical fluctuating voltage $\delta V_{\rm cl}(t)$ to the bias applied to the Josephson junction, such that $4e^2\langle\delta V_{\rm cl}(t)\delta V_{\rm cl}(t')\rangle = \Gamma_\varphi\delta(t-t')$. The Hamiltonian from Eq.(9) of the main text now reads:

$$\hat{\mathcal{H}}_{\rm RWA} = \frac{E_J}{2} e^{2ie\int^t dt'\delta V_{\rm cl}(t')} \sum_{n_{\rm s},n_{\rm aux}} w_{n_{\rm aux}+1,n_{\rm aux}}[\lambda_{\rm aux}]$$
$$w_{n_{\rm s}+1,n_{\rm s}}[\lambda_{\rm s}](|n_{\rm aux}+1\rangle\langle n_{\rm aux}| \otimes |n_{\rm s}+1\rangle\langle n_{\rm s}| + \text{H.c.}) \quad (1)$$

It is convenient to make a change of gauge which converts this fluctuating voltage into an equivalent fluctuating cavity frequency; such a fluctuating frequency will cause an equivalent decoherence of coherences in the cavity density matrix. The gauge change is done using the unitary operator $\hat{U} = \exp(-2ie\int^t dt'\delta V_{\rm cl}(t')\hat{a}_{\rm i}^\dagger\hat{a}_{\rm i})$ with i = s or aux. One can gauge the voltage noise into either the storage or cavity frequency, as both choices lead to equivalent decoherence of relevant density matrix coherences. We chose i = s. In the new gauge, the storage cavity has a fluctuating frequency:

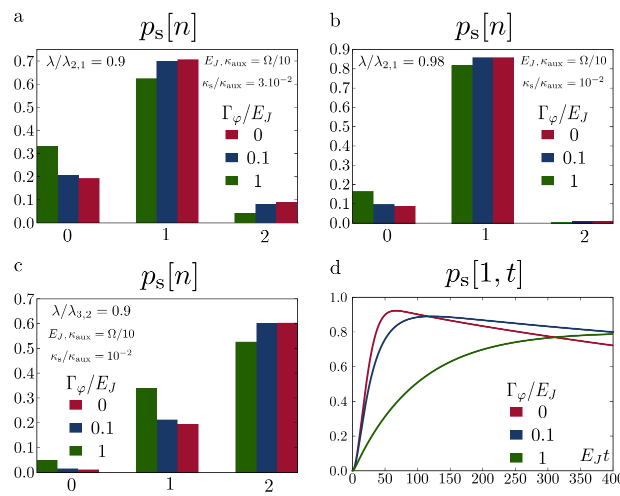

FIG. 1. (a-c) Steady-state probability $p_{\rm s}[n]$ for the storage cavity to be in a Fock state $|n\rangle$, as obtained from the RWA master equation (Eq.(10) of the main text) with the addition of a decoherence term describing voltage fluctuations (c.f. Eq. (3)); results for various decoherence rates Γ_φ are shown. (d) Time dependence of storage cavity photon number occupancy $p_{\rm s}[1,t]$, for various decoherence rates Γ_φ. Even for very large decoherence rates ($\Gamma_\varphi \simeq E_J \simeq 1$GHz), the low-frequency voltage fluctuations of the environment have negligible effects on the results presented in the main text.

$$\hat{\mathcal{H}}_{\rm RWA} = 2e\delta V_{\rm cl}(t)\hat{a}_{\rm s}^\dagger\hat{a}_{\rm s} + \frac{E_J}{2}\sum_{n_{\rm s},n_{\rm aux}} w_{n_{\rm aux}+1,n_{\rm aux}}[\lambda_{\rm aux}]$$
$$w_{n_{\rm s}+1,n_{\rm s}}[\lambda_{\rm s}](|n_{\rm aux}+1\rangle\langle n_{\rm aux}| \otimes |n_{\rm s}+1\rangle\langle n_{\rm s}| + \text{H.c.}). \quad (2)$$

Averaging over these frequency fluctuations in the standard manner (for white, Gaussian fluctuations) leads to an additional dephasing superoperator in the master equation that causes the decay of coherences. It has the form:

$$\frac{d\rho}{dt}\Big|_{\rm noise} = \Gamma_\varphi\left(\hat{n}_{\rm s}\hat{\rho}\hat{n}_{\rm s} - \frac{1}{2}\left(\hat{n}_{\rm s}^2\hat{\rho} + \hat{\rho}\hat{n}_{\rm s}^2\right)\right). \quad (3)$$

where $\hat{n}_{\rm s}$ is the photon number operator for the storage cavity.

In Figs. 1(a-c), we plot the steady-state probability $p_{\rm s}[n]$ for the storage cavity to be in a Fock state $|n\rangle$ for different values of Γ_φ and different values of λ and κ corresponding to those of Figs. 4a, 4b and 5 of the main text. In Fig. 1a we plot the probability of stabilizing one photon for a 10% mismatch in λ (corresponding to light blue bars in Fig.4a of the main text).

Even for values much larger than we expect for Γ_φ (that is $\Gamma_\varphi \simeq E_J \simeq 1$GHz), voltage fluctuations have a rather negligible effect on our results. In fact, large amounts of dephasing have a positive effect, in that they suppress transitions into higher unwated Fock states.

In Fig. 1b, we plot the probability of stabilizing one photon for a 2% mismatch in λ (corresponding to the middle bars in Fig.4a of the main text). We see that as we decrease the mismatch in impedance, the effects of the low-frequency environment get smaller. In Fig. 1c, we plot the probability of stabilizing two photons for a 10% mismatch in λ (corresponding to the light green bars in Fig.4b of the main text) and conclude that decoherence still has a minor effect on stabilizing higher Fock states. Finally in In Fig. 1(d), we plot the time-dependent number occupancy of the storage cavity $p_{\rm s}[1,t]$ (corresponding to the light green curve of Fig.5 of the main text), for different values of Γ_φ. Looking back to Eq.(12) of the main text, we see that voltage fluctuations serve to effectively decrease Γ, the effective pumping rate from $|0,0\rangle$ to $|1,0\rangle$. Similarly, they decrease the effective transition rate from $|n,0\rangle$ to $|n+1,0\rangle$. In principle, this implies that one could use a smaller value of $\kappa_{\rm s}$ (as the principle reason for having a not-too-small $\kappa_{\rm s}$ is to prevent the population of higher Fock states). If one makes this change, the results with voltage fluctuations become even closer to those presented in the main text.